

Refractive index of the alkali halides. II. Effect of pressure on the refractive index of 11 alkali halides

P. G. Johannsen, G. Reiß, U. Bohle, J. Magiera, R. Müller, H. Spiekermann, and W. B. Holzapfel
Fachbereich Physik, Universität GH Paderborn, D-33095 Paderborn, Germany

(Received 27 June 1996; revised manuscript received 8 November 1996)

A recently developed comparative interferometric method for the determination of the refractive index at high pressures is applied to NaF, NaBr, NaI, KCl, KBr, KI, RbCl, RbI, CsCl, CsBr, and CsI. In the studied pressure range up to 12 GPa, the potassium and rubidium halides show a polymorphic phase transition from NaCl- to CsCl-type structure, accompanied by a discontinuous increase of the refractive index. The pressure data of the sodium and cesium halides are converted from pressure to density dependences by the help of ultrasonic equations of state. The refractive index of the sodium halides shows an almost linear density dependence, while the cesium halides exhibit strong nonlinear behavior. The constant joint-density-of-states (CJDOS) model, proposed in the first paper of this series, is used for the further analysis of the data. In the CJDOS model the density dependence of the dielectric function is related to the different behaviors of *s* and *d* conduction bands with density. While the almost linear behavior of the sodium halides can be understood by a competition of an increasing contribution of transitions to the *d* bands, and a decreasing contribution of transitions to the *s* conduction band, the nonlinear behavior of the cesium halides is predominantly caused by the closure of the band gap, with a *d*-band character of the lower conduction-band states. [S0163-1829(97)06111-0]

I. INTRODUCTION

The pressure dependence of the refractive index (RI) of various materials is of current interest.¹ Fabry-Pérot (FP) interferences between two parallel culets of the anvils in a diamond-anvil cell (DAC) are generally analyzed for this purpose. The use of a Fourier-transform (FT) spectrometer is thereby advantageous,² as the FP fringes in the spectrum are represented by peaks in the interferogram, which can be readily measured, and contain the information of the optical path length.

The density or stress dependence of the alkali halides (AH's) is of special interest, because this group of substances can be regarded as prototype for ionic materials, and a comparison of experimental RI data with the predictions of model calculations can serve as a critical test of the respective model.³⁻⁸ Furthermore, because of their special physical properties, AH's are used as optical window materials in various applications requiring a knowledge of the stress or density dependences of these properties.⁹⁻¹⁴

In Sec. II the experimental details are given. In Sec. III, results of diamond-anvil experiments for the pressure dependence of 11 AH's up to 12 GPa are presented. The RI of the potassium and rubidium halides in the CsCl-type structure are given thereby for the first time, to our knowledge.

For the conversion of these pressure-dependent data into density dependences, the respective equations of state (EOS) for the different materials are required. Phenomenological EOS, based on ultrasonic data for the bulk modulus and its pressure derivatives, can be used for the sodium and cesium halides. In Sec. IV the density dependence of the RI of these materials, which do not undergo phase transitions in the present pressure range, is presented. These density depen-

dences exhibit significant differences between those two groups which can be related to different density dependences of the respective band structures in the constant joint-density-of-states (CJDOS) model.⁸ Thereby the band-gap closure in the cesium halides is responsible for the observed nonlinearity in the density dependence of the RI in this group of materials.

II. EXPERIMENT

The FP interferences between the two parallel culets of the anvils in a DAC lead to fringe patterns in transmission spectra. The spacing between two fringe maxima on a wave-number scale is equal to $1/(2nd)$ for normal incidence. For a determination of the RI *n*, additional information on the sample thickness *d* is necessary, which can be a major problem in many cases. Moreover, the analysis of the fringe patterns may involve sophisticated calculations for the accurate determination of the fringe maxima.¹

Recently a method has been proposed by which the thickness problem is overcome by the use of a reference material, with the same thickness as the sample, and the measurement of the respective RI ratio. Furthermore, it was shown that the use of a FT spectrometer is advantageous for an analysis of interference fringes in transmission spectra.²

A periodic pattern in a spectrum is represented by a peak in the respective interferogram. The dispersion of the RI and the spectral response of the spectrometer affect the peak position and shape. For linear dispersion the peak maximum corresponds to an effective RI

$$n_{\text{eff}} = \bar{n} + E \frac{\partial n}{\partial E}. \quad (1)$$

\bar{n} is the RI for the photon energy of the maximum of the instrumental response function. A Bruker IFS 113v FT spectrometer with a tungsten halogen lamp was used, together with a Si:CaF₂ beamsplitter in the present experiments. The signal was detected by a liquid-N₂-cooled InSb detector. The RI dispersion of the materials under consideration in the present spectral range is small,^{2,8} and the assumption of a linear dispersion in Eq. (1) is a good approximation.

NaCl was used as a reference material in the present experiments. The density (or volume) dependence of the RI of NaCl was thoroughly discussed in the first paper of this series.⁸ Various experimental results are cited in this paper and can be brought into excellent agreement with theoretical considerations, taking into account the joint density of states of the AH's, and its variation with density (the CJDOS-model). The pressure-volume relation of NaCl, on the other hand, is one of the pressure standards, used in high-pressure physics.¹ Thus the pressure dependence of the RI of NaCl can be regarded as known with sufficient accuracy to serve as a standard for RI determination.

In most of the experiments the gasket hole diameter was 300 μm . Pressures were determined by the use of ruby fluorescence technique with a linear scale.¹⁵ Experiments were made with increasing pressures only. It turned out that with decreasing pressures large nonisotropic strains occurred because of plastic deformations of the gasket hole. Different sample geometries were used for the check of nonisotropic deformations in the upstroke experiments: parts of the experiments were made with the sample and reference materials placed side by side in the gasket hole. In other experiments the hole was first filled with NaCl, which was compressed to build a plane-parallel window. Then a centric hole of 150- μm diameter was drilled into this NaCl window, and filled with the sample material.

Measurements with LiF (not discussed in this paper) showed that nonisotropic strains occur when the gasket hole becomes unstable at the end of a pressure run. It is well known that such gasket instabilities are accompanied by large deviatoric stresses and, of course, occur preferably with high bulk modulus materials, as, e.g., LiF or NaF. For the other materials the results were reproducible with the different sample geometries, discussed above. Furthermore, different rubies, placed both in the sample and reference materials, generally indicated no additional pressure gradients.

The experiments were limited in pressure for different reasons: the FP signal decreased when the RI of the material became comparable to the RI of the diamonds. Another reason for the decrease of the FP signal was the deformation of the diamonds at higher pressures.

III. RESULTS

A. Sodium halides

The sodium halides show no polymorphic transition in the present pressure range. NaBr and NaI had to be dried. While the tendency of NaBr to be contaminated is not very large, NaI required preparation under a cold, dry nitrogen atmosphere. A double-hole technique was used: two holes of 150- μm diameter were drilled side by side into the gasket. The first hole was filled with NaCl at ambient conditions. Then the second hole was filled with NaI at low tempera-

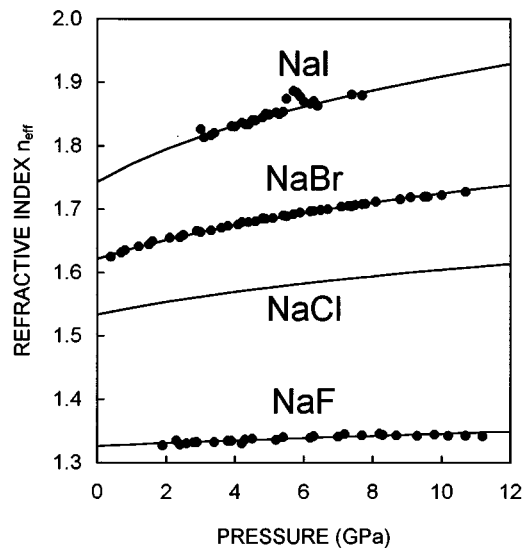


FIG. 1. Effect of pressure on the refractive index of sodium halides. The curves correspond to the CJDOS model with the parameters of Table I.

tures. The experimental results are shown in Fig. 1. The smooth curves were calculated with the help of the CJDOS model together with ultrasonic equations of state, as described in Sec. IV.

B. Potassium halides

KCl, KBr, and KI show polymorphic phase transitions from NaCl-type (B1) to CsCl-type (B2) structures at about 2 GPa.¹⁶ These phase transitions are accompanied by a volume decrease, and the samples change into an opaque form at first. With increasing pressure the materials become transparent, again permitting measurements of the RI in the B2 phase as well. The corresponding results are shown in Fig. 2.

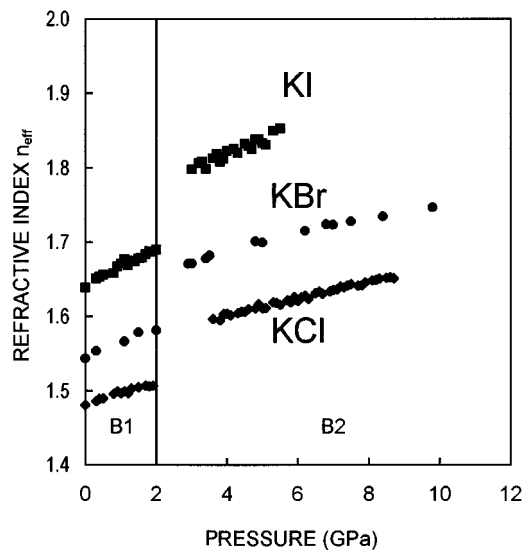


FIG. 2. Effect of pressure on the refractive index of potassium halides. The phase transition from the NaCl-type (B1) phase to the CsCl-type (B2) phase is accompanied by a discontinuous increase of the refractive index (see text).

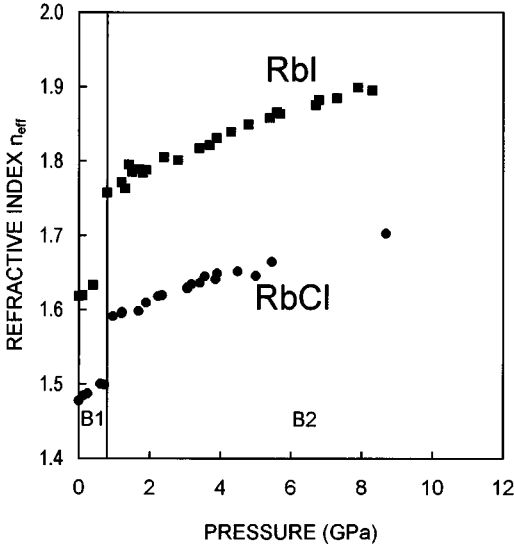


FIG. 3. Effect of pressure on the refractive index of rubidium halides. The phase transition from the NaCl-type ($B1$) phase to the CsCl-type ($B2$) phase is accompanied by a discontinuous increase of the refractive index.

The relative increase in density $\rho_{B2}/\rho_{B1}|_{p=2 \text{ GPa}}$ is 1.14, 1.13, and 1.11 for KCl, KBr, and KI, respectively. If one extrapolates the RI data for both phases to 2 GPa one obtains, for the ratios

$$(n_{B2}^2 - 1)/(n_{B1}^2 - 1)|_{p=2 \text{ GPa}}, \quad (2)$$

values which are slightly larger, namely, 1.15, 1.15, and 1.14, respectively. However, within the uncertainties of the extrapolations and the uncertainties of the experimental data for the density ratios, both ratios can be considered to be equal.

For a more detailed analysis of the data, especially for a discussion of the density dependencies, accurate EOS data are indeed required. With corresponding recent data,^{17,18} these density dependencies of the potassium halides will be discussed in a later paper.¹⁹

C. Rubidium halides

The behavior of the rubidium halides is very similar to the behavior of the potassium halides, with the difference that the phase transitions occur below 1 GPa. Only RbCl and RbI have been measured up to now. The corresponding experimental results are given in Fig. 3, and the density dependencies will be discussed together with the potassium halides later.

D. Cesium halides

Compared to the other halides the cesium halides exhibit a CsCl-type structure at ambient conditions, and no phase transitions occur in the present pressure range. A glance at the results in Fig. 4 shows that the behavior of the RI is different for the cesium halides compared to the results for the other halides. The pressure dependence is almost linear, and therefore points to a significant curvature of the density

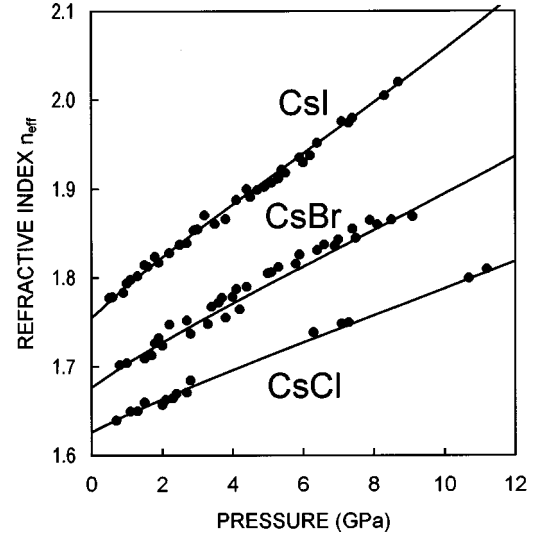


FIG. 4. Effect of pressure on the refractive index of cesium halides. The curves correspond to the CJDOS model with the parameters of Table III.

dependence of the cesium halides. The calculated curves in Fig. 4 correspond to the CJDOS model, with ultrasonic EOS data as discussed in Sec. IV.

IV. DENSITY DEPENDENCE

A. Sodium halides

For the conversion of the pressure dependence of the RI data into a density dependence, the EOS of the respective material is required. A lattice-dynamical model of Born type,^{20,21} with parameters based on ultrasonic data for the bulk modulus K_0 (Refs. 22 and 23) gives a good description for the EOS of the $B1$ phase of the AH's,¹⁸ and is used here for the conversion of the pressure dependence of the RI into the density dependence. The result is shown in Fig. 5. The curves are given by the function

$$n_{\text{eff}}(\rho) = \bar{n}(\rho) + E \left. \frac{\partial n}{\partial E}(\rho) \right|_{E=0.65 \text{ eV}}, \quad (3)$$

with

$$n(E, \rho) = \sqrt{1 + \Delta\epsilon_1^{\text{el}}(E, \rho) + \Delta\epsilon_1^{\text{TO}}(E, \rho)}. \quad (4)$$

$\Delta\epsilon_1^{\text{el}}$ and $\Delta\epsilon_1^{\text{TO}}$ are the electronic and phonon contributions to the dielectric function,⁸ and $\bar{n}(\rho) = n(0.65 \text{ eV}, \rho)$. The three energy parameters of the CJDOS model⁸ for NaF, NaBr, and NaI have been obtained by fitting Eq. (4) to the experimental data. These values are given in Table I together with the optical and EOS parameters required for the calculation of these curves.

The parameter E_{d0} represents the onset of transitions to the d bands in the CJDOS model. For NaF the value of 37 eV is somewhat higher than that of 29 eV obtained from band-structure calculations.²⁴ However, the fact that a gap between the s and d conduction bands is obtained in the CJDOS model is in good agreement with theory. As in LiF,⁸

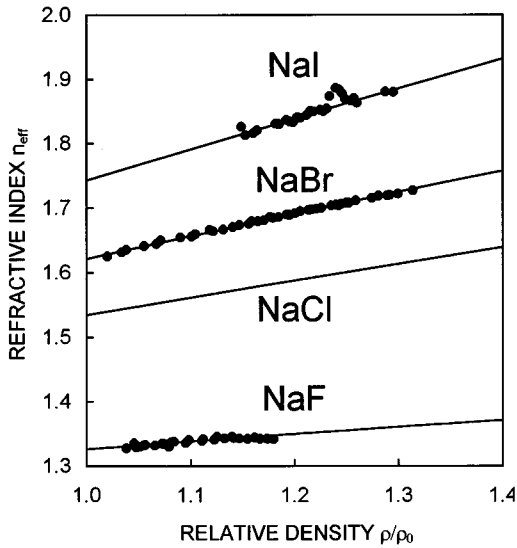


FIG. 5. Density dependence of the refractive index for sodium halides. The curves correspond to the CJDOS model with the parameters of Table I.

the constituent ions in NaF have no low-lying d levels, and transitions to the d bands thus only make a small contribution to the dielectric function.

In NaBr and NaI the d bands have much lower energies, similar to the situation in NaCl,⁸ and contribute to the JDOS. The present value $E_{d0}=11$ eV for NaBr (Table I) is quite close to the calculated value 12 eV.²⁵ For NaI, some overlap of s and d bands is predicted.

In the present density range the RI of the sodium halides shows an almost linear behavior (Fig. 5). In the CJDOS model this is mainly caused by the competition of the different contributions of s and d bands. While the opening of the p - s gap favors a slightly sublinear behavior, as, e.g., in LiF,⁸ the closing of the p - d gap is accompanied by a steeper increase of the RI (e.g., in the cesium halides, see below). Table II gives the density derivative for some selected energies, calculated with Eq. (4) and the data in Table I.

B. Cesium halides

Ultrasonic parameters K_0 , K'_0 , and K''_0 for CsCl, CsBr, and CsI have been determined in Ref. 26. The authors propose to use the parameters in connection with a second-order Birch EOS,²⁷ which they found to be in good agreement with early volumetric data^{28,29} and a Born-model EOS. In the meantime, more experimental and theoretical data have be-

TABLE I. CJDOS parameters for the calculation of the curves in Figs. 1 and 5.

	n_∞^a	E_{x0}^a (eV)	E_{c0} (eV)	E_{d0} (eV)
NaF	1.3210	10.87	17.63	36.75
NaCl	1.5278	7.58	12.40 ^a	14.10 ^a
NaBr	1.6126	6.49	9.77	11.09
NaI	1.7305	5.62	8.15	7.83

^aReference 8.

TABLE II. Dispersion of the density derivative of the refractive index of the sodium halides.

E (eV)	$\rho \partial n / \partial \rho$			
	0	1	2	3
NaF	0.124	0.122	0.120	0.116
NaCl	0.276	0.274	0.268	0.254
NaBr	0.360	0.358	0.350	0.329
NaI	0.490	0.489	0.483	0.461

come available, and are in reasonable agreement with the proposed EOS in the present pressure range.¹⁸

In Fig. 6 the density dependences of the RI, obtained with these EOS's, are shown. The most striking difference compared to the results of the sodium halides is the positive curvature. For CsI it has been shown that band-gap closure is responsible for this density dependence, and the experimentally determined variation of the gap has been used to obtain the density dependence of the CJDOS parameter E_d ,⁸

$$E_d(\rho) = E_{d0} \left[1 + \gamma_d \frac{\Delta \rho}{\rho_0} + \delta \left(\frac{\Delta \rho}{\rho_0} \right)^2 \right], \quad (5)$$

with $\gamma_d = -\frac{1}{3}$ and $\delta = -0.576$. For the calculation of the curves in Fig. 6, the same variation of the gap has also been assumed for CsCl and CsBr. The other required parameters are given in Table III. The dispersion of the density derivative is given in Table IV.

V. DISCUSSION

There is no universal method for a determination of the refractive index at high pressures for every substance. The present experimental method² has been successfully applied to 11 alkali halides, and has shown its advantages for this group of substances. The major disadvantage of the method is of course its limitation to rather soft and optically isotropic

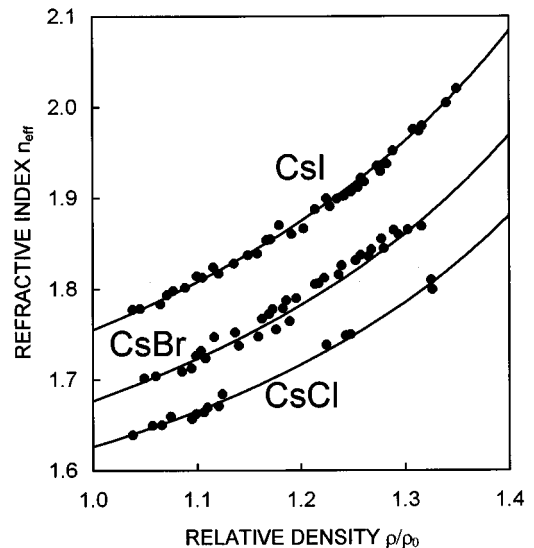


FIG. 6. Density dependence of the refractive index for cesium halides. The curves correspond to the CJDOS model with the parameters of Table III.

TABLE III. CJDOS parameters for the calculation of the curves in Figs. 4 and 6.

	n_{∞}^a	E_{x0}^a (eV)	E_{c0} (eV)	E_{d0} (eV)
CsCl	1.6190	7.49	22.17	8.27
CsBr	1.6686	6.67	14.56	7.34
CsI	1.7428	5.65	10.66 ^a	6.41 ^a

^aReference 8.

samples¹ with RI, which are different from the RI of diamond. However, for such materials the method seems superior to any other known method. The major advantages are the following.

(1) The preparation of the DAC is rather simple, and cryogenic loading can be applied in the case of hygroscopic samples.

(2) It is possible to measure the refractive index in high pressure phases, as has been demonstrated for the potassium and rubidium halides.

(3) The use of a FT spectrometer is advantageous in any case because no mathematical calculations are required for the determination of the relative RI.

It has been noted¹ that the use of an interferometer “seems unsuitable for measurements on samples placed in a hydrostatic medium in the cavity of a DAC.”³⁰ “In this case,” goes the argument in Ref. 1, “there are many interference cavities and spurious peaks appear in the interferogram, making assignment difficult.” This argument does not hold true. On the contrary, the interferogram can be much more easily interpreted than the respective spectrum in the case of several interference cavities, because the assignment is very simple: the peaks occur according to their optical thicknesses, and can be identified from their positions at am-

TABLE IV. Dispersion of the density derivative of the refractive index of the cesium halides.

E (eV)	$\rho \partial n / \partial \rho$			
	0	1	2	3
CsCl	0.351	0.352	0.354	0.358
CsBr	0.416	0.417	0.420	0.426
CsI	0.474	0.475	0.479	0.481

bient conditions and easily followed in a pressure run. Even in the case when a conventional spectrometer has been used to measure the interference pattern, the Fourier transformation, using an available fast-Fourier-transform algorithm, can be performed with less mathematical effort than the much more tedious simulation of the spectrum.³⁰ An important point in this connection is the fact that interference peaks from very thin cavities, which are not of interest in most cases, appear near the center burst of the interferogram, and are not resolved.

It has been shown that the CJDOS model⁸ gives an excellent description not only for the RI dispersion of the AH's, but also for the density dependences. Within this model the RI is strongly related to the behavior of s and d bands. The competition between the shift of the s excitons to higher energies, and the closing of the p - d gap in the sodium halides, leads to an almost linear density dependence of the RI, while the closing of the band gap in the cesium halides shows up in a nonlinear behavior.

For an interpretation of the potassium and rubidium data in their high-pressure phase, accurate EOS data are required. Such data are now available,^{17,18} and the density dependence of the RI of the potassium and rubidium halides will be given in a later paper.¹⁹

¹M. I. Eremets, *High Pressure Experimental Methods* (Oxford University Press, Oxford, 1996), and references therein.

²P. G. Johannsen, *Meas. Sci. Technol.* **4**, 237 (1993).

³J. N. Wilson and R. M. Curtis, *J. Phys. Chem.* **74**, 187 (1970).

⁴H. Coker, *J. Phys. Chem. Solids* **40**, 1079 (1979).

⁵S. H. Wemple and M. DiDomenico, *Phys. Rev. B* **3**, 1338 (1971).

⁶J. Van Vechten, *Phys. Rev.* **182**, 891 (1969).

⁷J. Shanker, G. G. Agrawal, and N. Dutt, *Phys. Status Solidi B* **138**, 9 (1986).

⁸P. G. Johannsen, *Phys. Rev. B* **55**, 6856 (1997).

⁹B. Bendow, P. D. Gianino, Y. F. Tsay, and S. S. Mitra, *Appl. Opt.* **13**, 2382 (1974).

¹⁰K. Vedam, E. D. D. Schmidt, and W. C. Schneider, in *Optical Properties of Highly Transparent Solids*, edited by S. S. Mitra and B. Bendow (Plenum, New York, 1975), p. 169.

¹¹S. B. Kormer, *Usp. Fiz. Nauk* **94**, 641 (1964) [*Sov. Phys. Usp.* **11**, 229 (1968)].

¹²J. L. Wise and L. C. Chhabildas, in *Shock Waves in Condensed Matter*, edited by Y. M. Gupta (Plenum, New York, 1986), p. 441.

¹³J. Wackerle and H. L. Stacy, in *Shock Waves in Condensed Mat-*

ter, edited by S. C. Schmidt and N. C. Holmes (Elsevier, Amsterdam, 1988), p. 699.

¹⁴A. L. Ruoff and K. Ghandehari, in *High-Pressure Science and Technology*, AIP Conf. Proc. No. 309 (AIP, New York, 1994), p. 1523.

¹⁵G. J. Piermarini, S. Block, J. D. Barnett, and R. A. Forman, *J. Appl. Phys.* **46**, 2774 (1975).

¹⁶*American Institute of Physics Handbook*, 3rd ed (McGraw-Hill, New York, 1972).

¹⁷U. Köhler, P. G. Johannsen, and W. B. Holzapfel, *J. Phys. Condens. Matter* (to be published).

¹⁸P. G. Johannsen (unpublished).

¹⁹P. G. Johannsen (unpublished).

²⁰M. Born and K. Huang, *Dynamical Theory of Crystal Lattices* (Clarendon, Oxford, 1954).

²¹M. P. Tosi, in *Solid State Physics*, edited by F. Seitz and D. Turnbull (Academic, New York, 1964), Vol. 16, p. 1.

²²R. W. Roberts and C. S. Smith, *J. Phys. Chem. Solids* **31**, 619 (1970).

²³C. S. Smith and L. S. Cain, *J. Phys. Chem. Solids* **36**, 205 (1975).

²⁴F. Perrot, *Phys. Status Solidi B* **52**, 163 (1972).

²⁵A. B. Kunz and N. O. Lipari, *Phys. Rev. B* **4**, 1374 (1971).

²⁶G. R. Barsch and Z. P. Chang, in *Accurate Characterization of the High-Pressure Environment*, edited by E. C. Lloyd, Natl. Bur. Stand. (U.S.) Spec. Publ. No. 326 (U.S. GPO, Washington, DC, 1971), p. 173.

²⁷F. Birch, *J. Geophys. Res.* **57**, 227 (1952).

²⁸P. W. Bridgman, *Proc. Am. Acad. Sci.* **74**, 21 (1940).

²⁹P. W. Bridgman, *Proc. Am. Acad. Sci.* **76**, 1 (1945).

³⁰J. H. Eggert, L. W. Xu, R. Z. Che, L. C. Chen, and J. F. Wang, *J. Appl. Phys.* **72**, 2453 (1992).